Journal of Computational Interdisciplinary Sciences (2013) 4(1): 23-33

Printed version ISSN 1983-8409 / Online version ISSN 2177-8833
http://epacis.net
doi: 10.6062/jcis.2013.04.01.0067

Hydrodynamic transfer function associated to a Rotating Disk Electrode in the presence of a viscosity gradient

N.A. Leite[1], O.E. Barcia[1,3], O.R. Mattos[1], J. Pontes[1] and N. Mangiavacchi[2]

Manuscript received on March 14, 2013 / accepted on April 12, 2013

ABSTRACT

This work investigates the behaviour of the hydrodynamic transfer function of Rotating Disk Electrode (RDE) obtained with the hydrodynamic and mass transfer equations coupled through the dependency of the viscosity on the concentration of a chemical species in the electrolyte, which originates from the dissolution of iron electrodes in the $\mathbf{1M\ H_2SO_4}$ electrolyte solution. The results are compared with those obtained for constant viscosity and for the case where a viscosity profile depending on the distance to the electrode surface is imposed, decoupling the hydrodynamic and mass transfer equations. The results show that the existence of a viscosity gradient in the neighborhood of the RDE affects the hydrodynamic transfer function and changes increase with the increase of the perturbation frequency imposed to the angular velocity of the electrode. The coupling between the concentration and the hydrodynamic fields introduces a dependency of the transfer function on the Schmidt number. And higher viscosity gradients, or Schmidt numbers reduce the phase angle delay of the transfer function for a given perturbation frequency p, in comparison with systems with constant viscosity.

Keywords: corrosion, electro-hydrodynamic impedance, rotating disk electrode.

1 INTRODUCTION

Rotating disk electrodes (RDE) have been widely used in kinectic studies related electrodeposition and electrodissolution of metals [1, 4], due to the simplicity of the experimental setup and of the simplifications made in the hydrodynamic and mass transport equations, taking into account the experimental conditions [1]. In this sense, for suitable values of the angular velocity imposed to the RDE the thickness of the diffusion boundary layer is sufficiently small when compared to the electrode radius, leading to a mass flux independent to the radial coordinate along the disk. Additionally, the ions transfer rate in the neigbouhood of the electrode is conveniently controlled by the imposed angular velocity. As far as the electrochemical kinetics is controlled by the mass transfer, the rate of mass transfer settles the maximum steady current attained in an experiment.

In 1983 Tribollet & Newman [5] developed a new electrochemical technique, denoted as electrochemical impedance (Z_{EHD}), which consists in modulating the angular velocity

Correspondence to: Nathália A. Leite – Email: natls@metalmat.ufrj.br
[1]Metallurgical and Materials Engineering Department, Escola Politécnica – Instituto Alberto Luis Coimbra de Pós-Graduação e Pesquisa, Federal University of Rio de Janeiro, Rio de Janeiro, Brazil.
[2]Mechanical Engineering Department/GESAR Group, State University of Rio de Janeiro, Rio de Janeiro, Brazil.
[3]Department of Physical Chemistry – Institute of Chemistry/Federal University of Rio de Janeiro, Brazil.

of the RDE with a second frequency. The sinusoidal current or potential response leads to the sought Z_{EHD} (defined as the product of the hydrodynamic and the mass transfer functions). Following the procedure previously adopted for steady systems [1], Tribollet & Newman [5] solved the electro-hydrodynamic impedance problem in two steps. In the first step, the authors used Newman's method [4, 6] to solve the unsteady hydrodynamic problem, by numerically integrating the time-dependent continuity and Navier-Stokes equations. Having solved the steady and unsteady hydrodynamic equations, Tribollet & Newman [5] addressed, in a second step the unsteady mass transfer problem obtained a solution in form of a power series containing the Schmidt number (Sc) raised to the power –1/3. Finally, the authors obtained the Z_{EHD}, from the solution of the hydrodynamic and mass transfer problems [5].

By using the concept of electro-hydrodynamic impedance Barcia *et al.* addressed the problem of the anodic dissolution of the iron in the region where the electrodissolution is fully controlled by the mass transfer [7]. Since the current control by the mass transfer assumes saturation of the Fe^{2+} concentration at the electrode surface, many authors assume that an iron sulfide film covers the electrode [8, 9]. However, by using the Z_{EHD} Barcia *et al.* that the electrode surface is uniformly accessible in the region where the anodic dissolution kinetics is controled by the mass transfer process [7]. In addition, the experimental results obtained by these authors show the phase limit of the Z_{EHD} attained 180° at a frequency value different from the one proposed by Tribollet & Newman for an uniformly accessible surface [5]. In an effort to explain the phenomenon Barcia *et al.* assumed the existence of a viscosity gradient at the electrode interface [7] and proposed an empirical expression describing the viscosity profile along the axial coordinate and followed the procedure adopted by Tribollet & Newman [5], solving first the hydrodynamic problem with the assumed viscosity profile given by Eq. 19, and proceeded with the numerical integration of the unsteady mass transport equation [7].

The hypothesis about the existence of viscosity profile close to the electrode surface, in a potential regime where the kinetics is fully controlled by the mass transfer sounds consistent. By considering that a concentration gradient occurs at this level of applied potential it seems likely that a viscosity profile exists, having in mind that the viscosity depends on the concentration of this solution [10, 11]. However, as a corolary, the hydrodynamic equations depend on the concentration no longer can be solved independently of the convection-diffusion equation. Actually, these equations must be solved simultaneously and an additional equation, relating the viscosity to the concentration.

An empirical law coupling both fields was first proposed by Calabrese Barton & West [12] to simultaneously solve the hydrodynamic and mass transfer problems in order to cope with the experimental, the steady limit current and electro-hydrodynamic impedance of the $Zn-KOH$ system. In this work, the authors introduced the following equation [12]:

$$\frac{\nu(z)}{\nu(\infty)} = 1 + \left[\frac{\nu(0)}{\nu(\infty)} - 1\right]\theta^{\alpha} \qquad (1)$$

where $\nu(z)$ is the electrolyte viscosity dependent on the axial distance z to the electrode surface, $\nu(\infty)$ is the bulk viscosity, θ is the nondimensional concentration, and α is an empirical parameter. We can see that, for non uniform viscosity $\nu(0)/\nu(\infty) \neq 1$. α ranged from 1 to 3, and the viscosity ratio, $(\nu(0)/\nu(\infty))$, from 5.5 to 2.1, respectively. According to the authors, though the non uniform viscosity model was supported by strong experimental evidence adherence to the experimental data was not satisfactory, leading the authors to guess that additional features should be added to the model, like assuming the Stokes-Einstein law, or a simple power law relating viscosity to the concentration. We emphasize that Eq. 1 contains two unknown parameters, $\nu(0)$ and α.

Recently, Barcia *et al.* [13] solved the steady problem of the RDE assuming the Stokes-Einstein equation, as Calabrese Barton & West [12] did, but following a different approach to relate viscosity to the concentration. Barcia *et al.* [13] as well as Pontes *et al.* [14], assumed a simplified version of an exponential law relating both variables, derived by Esteves [11]. This simplified version is given by Eq. 26.

This work investigates the behaviour of the RDE hydrodynamic transfer function with the hydrodynamic and mass transfer equations coupled through Eqs. 11-13 and 24. The results are compared with those obtained for constant viscosity and for the case where a viscosity profile depending on the distance to the electrode surface is imposed, decoupling the hydrodynamic and mass transfer equations. Of course, the analysis of the coupled fields can be extended for the non steady situation in future. A complete model coupling the hydrodynamic and mass transfer equations for both steady and non steady conditions is currently under development in our group.

2 MATHEMATICAL MODEL

The continuity and Navier-Stokes equations, applicable to flow close to a RDE of an electrolyte with viscosity depending on the axial coordinate read [14]:

$$\frac{\partial v_r}{\partial r} + \frac{v_r}{r} + \frac{\partial v_z}{\partial z} = 0 \tag{2}$$

$$\frac{\partial v_r}{\partial t} + v_r\frac{\partial v_r}{\partial r} - \frac{v_\theta^2}{r} + v_z\frac{\partial v_r}{\partial z} = \nu\left[\frac{2}{r}\frac{\partial}{\partial r}\left(r\frac{\partial v_r}{\partial r}\right) - \frac{2v_r}{r^2}\right] + \frac{\partial}{\partial z}\left(\nu\frac{\partial v_r}{\partial z}\right) \tag{3}$$

$$\frac{\partial v_\theta}{\partial t} + v_r\frac{\partial v_\theta}{\partial r} + \frac{v_r v_\theta}{r} + v_z\frac{\partial v_\theta}{\partial z} = \frac{\nu}{r^2}\frac{\partial}{\partial r}\left[r^3\frac{\partial}{\partial r}\left(\frac{v_\theta}{r}\right)\right] + \frac{\partial}{\partial z}\left(\nu\frac{\partial v_\theta}{\partial z}\right) \tag{4}$$

where z, r, v_r, v_θ and v_z stand for their classical meaning.

The above equations can be written in nondimensional form as follows: according to Tribollet & Newman [5], the instantaneous angular velocity Ω is defined by:

$$\Omega = \bar{\Omega} + \Delta\Omega\,\mathrm{Re}\{e^{j\omega t}\} \tag{5}$$

where the overbar designates the steady state. For low modulation amplitudes ($\Delta\Omega \ll \bar{\Omega}$) and generalizing the classical von Kármán transformation [15], we can write:

$$v_r = r\bar{\Omega}\left[F(\xi) + \frac{\Delta\Omega}{\bar{\Omega}}\mathrm{Re}\{\tilde{f}(\xi)e^{j\omega t}\}\right] \tag{6}$$

$$v_\theta = r\bar{\Omega}\left[G(\xi) + \frac{\Delta\Omega}{\bar{\Omega}}\mathrm{Re}\{\tilde{g}(\xi)e^{j\omega t}\}\right] \tag{7}$$

$$v_z = \sqrt{\nu\bar{\Omega}}\left[H(\xi) + \frac{\Delta\Omega}{\bar{\Omega}}\mathrm{Re}\{\tilde{h}(\xi)e^{j\omega t}\}\right] \tag{8}$$

where ξ is a nondimensional distance defined by:

$$\xi = z\left[\frac{\Omega}{\nu(\infty)}\right]^{1/2} \tag{9}$$

and F, G, H, $\tilde{f}$, $\tilde{g}$ and $\tilde{h}$ are nondimensional profiles, with $\tilde{f}$, $\tilde{g}$ and $\tilde{h}$ being complex functions.

Upon substituting Eqs. 6-9, in Eqs. 2-4 and defining the nondimensional viscosity $\nu^*(\xi)$ as:

$$\nu^*(\xi) = \frac{\nu(z)}{\nu(\infty)}, \tag{10}$$

with $\nu(z)$ being the local viscosity and $\nu(\infty)$, the bulk viscosity, we obtain two systems of equations, the first one applicable to the steady state:

$$2F + H' = 0 \tag{11}$$

$$F^2 - G^2 + HF' - \nu^*F'' - \nu^{*\prime}F' = 0 \tag{12}$$

$$2FG + HG' - \nu^*G'' - \nu^{*\prime}G' = 0 \tag{13}$$

and the second one for the nonsteady flow:

$$2\tilde{f} + \tilde{h}' = 0 \tag{14}$$

$$jp\tilde{f} + 2F\tilde{f} - 2G\tilde{g} + H\tilde{f}' + F'\tilde{h} - \nu^{*\prime}\tilde{f}' - \nu^*\tilde{f}'' = 0 \tag{15}$$

$$jp\tilde{g} + 2\tilde{f}G + 2F\tilde{g} + G'\tilde{h} + H\tilde{g}' - \nu^{*\prime}\tilde{g}' - \nu^*\tilde{g}'' = 0. \tag{16}$$

In both systems, prime stands for derivatives with respect to ξ, and $p = \omega/\bar{\Omega}$ is the nondimensional modulating frequency in Eqs. 15 and 16. Boundary conditions are:

$$\begin{aligned} &F(0) = H(0) = 0 \\ &G(0) = 1 \\ &F(\infty) = G(\infty) = 0 \end{aligned} \tag{17}$$

for the system represented by Eqs. 11-13, and

$$\begin{aligned} &\tilde{f}(0) = \tilde{h}(0) = 0 \\ &\tilde{g}(0) = 1 \\ &\tilde{f}(\infty) = \tilde{g}(\infty) = 0 \end{aligned} \tag{18}$$

for the system represented by Eqs. 14-16.

Taking into account the existence of a viscosisty gradient pointing from the RDE surface, namely, $\nu^* \neq 1$ and $(\nu^*)' \neq 0$, two possible approaches may be envisaged to solve the above equations. In the first one a viscosity profile depending on the distance form the electrode surface ξ is assumed. Barcia *et al.* [7] assumed the following profile, based on which the resulting solution of the hydrodynamic and transport equations lead to results consistent with the experimental data:

$$\frac{\nu(\xi)}{\nu(\infty)} = \frac{\nu(0)}{\nu(\infty)} + \left(1 - \frac{\nu(0)}{\nu(\infty)}\right)\left(\frac{15}{\Gamma(4/3)}\right)\int_0^\xi e^{(-15\xi)^3}\mathrm{d}\xi. \tag{19}$$

where Γ is the gamma function [19].

A second approach consists in assuming that the variable viscosity results from the concentration profile at the electrode-electrolyte interface. Accordingly, the anodic dissolution process gives raise to a concentration gradient in compliance with Eqs. 11-13. The concentration profile leads to the viscosity gradient, which affects the hydodynamic field in the neighborhood of the RDE, further changing the concentration profile and again, the viscosity profile. The process repeats towards a new steady state profiles are attained. By following this approach, Barcia *et al.* [13], simultaneously solved Eqs. 11-13 coupled to the mass transfer equation given by:

$$v_z \frac{\partial c}{\partial z} = \frac{\partial D}{\partial z}\frac{\partial c}{\partial z} + D\frac{\partial^2 c}{\partial z^2} \tag{20}$$

where $c(z)$ are $D(z)$ represent the concentration and the diffusion coeficient at distance z from the electrode surface. We define the nondimensional concentration by:

$$\theta(\xi) = \frac{c(z) - c(\infty)}{c(0) - c(\infty)} \tag{21}$$

where $c(0)$ and $c(\infty)$ are the interface and bulk concentrations, respectively.

Assuming the Stokes-Einstein equation, $\nu D =$ constant, we can write:

$$\nu(z)D(z) = \nu(\infty)D(\infty) \tag{22}$$

where $D(\infty)$ is the bulk diffusion coefficient. Similarly, we define a nondimensional diffusion coefficient by:

$$D^*(\xi) = \frac{D(z)}{D(\infty)}. \tag{23}$$

By following the same nondimensionalization procedure adopted for the hydrodynamic equations 11-13 and taking into account Eqs. 21-23, we obtain the nondimensional form of Eq. 20

$$ScH\theta' - \frac{\theta'}{\nu^*} + \frac{\nu^{*\prime}}{(\nu^*)^2}\theta' = 0 \tag{24}$$

where Sc is the Schmidt number, given by $Sc = \nu(\infty)/D(\infty)$, and prime represents differentiation with respect to ξ. Boundary conditions for this equation are given by:

$$\begin{aligned} \theta(0) &= 1 \\ \theta(\infty) &= 0 \end{aligned} \tag{25}$$

Solving the coupled equations 11-13 and 24, with boundary conditions given by Eqs. 17 and 25 requires that the relation between viscosity and concentration be known. As already mentioned here we assume a simplified version of a constitutive equation previously derived by Esteves [11]. This simplified equation reads:

$$\frac{\nu(z)}{\nu(\infty)} = \exp\left[m\frac{c(z) - c(\infty)}{c(0) - c(\infty)}\right]. \tag{26}$$

Here, $m = \ln[\nu(0)/\nu(\infty)]$ is a parameter depending on the interfacial concentration only. Equation 26 may be written in nondimensional form as follows:

$$\nu^*(\xi) = \exp[m\,\theta(\xi)] \tag{27}$$

where $\nu^*(\xi)$ and $\theta(\xi)$ are given by Eqs. 10 and 21, respectively. Equation 27 introduces a dependency between viscosity and concentration, requiring thus, that the continuity, Navier-Stokes mass transfer equations be solved simultaneously. When $m = 1$, no viscosity gradient exists at the RDE interface, so Eqs. 11-13 and 24 can be solved independently.

In both cases, after solving the steady state hydrodynamic equations we solve the non steady equations 14-16 in order to obtain the RDE hydrodynamic transfer function defined and presented in [20].

Both in the steady and in the non steady cases the equations are numerically solved in a staggered grid of uniformly spaced points, using second-order finite-difference approximations for the derivatives.

3 RESULTS

3.1 Stationary Results

Solving Eqs. 11-13 and 24, with boundary conditions given by Eqs. 17 and 25, requires that the bulk Schmidt number Sc and parameter m are known. Having in mind that the Schmidt is given by $Sc = \nu(\infty)/D(\infty)$ and that $m = \ln[\nu(0)/\nu(\infty)]$, according to Eq. 26 we conclude that the governing equations cannot be solved in general form. The particular experimental setup must be prescribed. The particular electrolyte solution considered defines the associated values of $\nu(\infty)$ and $D(\infty)$ and consequently, the Schmidt number. The experimental setup does not defines the particular value of m. Evaluation of m requires additional experimental data for each particular run.

Having in mind that evaluation of the hydrodynamic transfer function, does not require solving Eq. 24, prescription of the Schmidt number is not required in two cases, when $m = 1$ and the viscosity gradient vanishes, or when an expression for the gradient is known *a priori*. However, even in this last case, though Eq. 26 can be dropped a value for the ratio $\nu(0)/\nu(\infty)$ must be assumed.

Table 1 – $\nu(0)/\nu(\infty)$ for $Sc(\infty) = 1500$, 2000 and 2200 and, for each value of $Sc(\infty)$, $c(0) = 1{,}8$M and 2,2M.

Sc=1500		Sc=2000		Sc=2200	
$c(0)(M)$	$\nu(0)/\nu(\infty)$	$c(0)(M)$	$\nu(0)/\nu(\infty)$	$c(0)(M)$	$\nu(0)/\nu(\infty)$
1.8	1.8	1.8	1.6	1.8	1.2
2.2	2.5	2.2	2.255	2.2	1.7

In the present paper we evaluate the hydrodynamic transfer function in both conditions and also, by assuming the coupling between the steady concentration and hydrodynamic fields and values must be assined to the Schmidt number Sc and m. The particular experimental setup and the operating conditions must be given.

As above said, we assume a system where anodic dissolution of iron in a 1M H_2SO_4 solution occurs, in a regime where dissolution kinetics is fully controlled by the mass transfer [7]. The interfacial and bulk Schmidt number for this particular system are approximately $Sc(0) = 8000$ and $Sc(\infty) = 2000$, respectively, for an interfacial concentration of Fe^{+2} (the electroactive species) $c(0) = 1.8$M [7]. In addition, the current density is given by:

$$i = nF\left(\frac{1}{Sc}\right)\left(\frac{1}{\nu(0)/\nu(\infty)}\right) \times \left[c(\infty) - c(0)\right]\sqrt{\nu(\infty)\bar{\Omega}}\left(\frac{d\theta}{d\xi}\right)_{\xi=0}, \tag{28}$$

in conditions where the electrodissolution process is controlled by mass transfer [7].

In order to investigate the effect of the bulk Schmidt number and of the interfacial concentration three Schmidt number, $Sc(\infty) = 1500$, 2000 and 2200, and concentration values given in Table 1 are assumed.

For example, assuming interfacial and bulk Schmidt numbers $Sc(0) = 8000$ and $Sc(\infty) = 2000$, and $c(0) = 1{,}8$M we have:

$$\frac{\nu(0)}{\nu(\infty)}\frac{D(\infty)}{D(0)} = 4. \tag{29}$$

According to the Stokes-Einstein equation $\nu D = $ constant, we have:

$$\nu(0)D(0) = \nu(\infty)D(\infty). \tag{30}$$

Thus:

$$\frac{D(\infty)}{D(0)} = \frac{\nu(0)}{\nu(\infty)} \tag{31}$$

By substituting this result in Eq. 29,

$$\frac{\nu(0)}{\nu(\infty)} = m = 2. \tag{32}$$

We have thus an approximate value for m, associated to $Sc(\infty) = 2000$. Based on these figures, Eqs. 11-13 and 24 are solved, with boundary conditions given by Eqs. 17 and 25, leading to the sought profiles F, G, H and θ. θ'(0) is then evaluated for $Sc = 2000$, $m = 2$ and $c(0) = 1{,}8$M, using the experimental corrent value in Eq. 28 to obtain a new value for m. With this value we solve again Eqs. 11-13 and 24 to evaluate m once more. The process is repeated until convergence is atained for the value of m. Schematically, we adopted the following procedure to solve the steady state equations:

1. Based on the experimental setup configuration and on previous experimental results we assume values for the RDE angular velocity (Ω), the Schmidt number (Sc), the bulk viscosity $\nu(\infty)$, the interfacial concentration $(c(0))$ and m, which defines the $\nu(0)/\nu(\infty)$ ratio.

2. The nondimensional profiles F, G, H and θ are obtained by numerically solving Eqs. 11-13, leading to a value for $\theta'(0)$.

3. The experimental value of the current i obtained by Barcia *et al.* [7], the angular velocity (Ω), the Schmidt number (Sc), the bulk viscosity $(\nu(\infty))$, the interfacial concentration $(c(0))$ and the result from item 2 $(\theta'(0))$ are inserted in Eq. 28. A new estimation of m is obtained and compared with the figure assumed to solve Eqs. 11-13.

4. Steps 1-3 are repeated with the new value of m, with the remaining parameters unchanged untill convergence for the value of m. An equivalent statement consists in saying that steps 1-3 are repeated until convergence is attained for the value of the current density. Acceleration of the process is obtained by using the Newton-Raphson method.

Table 1 shows the results obtained for several values of the interfacial/bulk viscosity ratios $[\nu(0)/\nu(\infty)]$ assuming $Sc(\infty)$ values 1500, 2000 and 2200 and $c(0)$ equal to 1.8M and 2.2M for each value of the Schmidt number.

Upon solving the uncoupled hydrodynamic and mass transfer equations and assuming $Sc(\infty) = 2000$ and $c(0) = 1.8$M, we obtain $\nu(0)/\nu(\infty) = 4.0$ [7]. Comparison with the results presented in Table 1, obtaind by soving the coupled equations show a difference, with $\nu(0)/\nu(\infty) = 1.6$ in the last case. From Table 1 we can see that the ratio $\nu(0)/\nu(\infty)$ decreases with the increase of the Schmidt number ($Sc(\infty)$) and increases with the interfacial concentration ($c(0)$). However, in all cases shown in Table 1 values below 4.0 are attained by the ratio $[\nu(0)/\nu(\infty)]$.

As discussed in Ref. [14] and in the results presented in Table 1, the coupling of the steady hydrodynamic and mass transfer equations lead to values of the ratio $[\nu(0)/\nu(\infty)]$ smaller than those previously assumed in the literature [6, 17, 18]. However the axial component of the steady state velocity (v_z or H) is strongly affected by the viscosity gradient [13]. In the next section we discuss how the non steady results change.

3.2 Non Steady Results

RDE hydrodynamic transfer function is defined as $\tilde{f}'(0, p)/\tilde{f}'(0, 0)$ [16]. Evaluation of this functions requires that Eqs. 14-16 with boundary conditions given by Eqs. 18 be solved. To accomplish the task we write each complex functions as a sum of two real functions:

$$\tilde{f} = f_1 + jf_2 \tag{33}$$

$$\tilde{g} = g_1 + jg_2 \tag{34}$$

$$\tilde{h} = h_1 + jh_2. \tag{35}$$

Inserting the above decomposition in Eqs. 14-16, we split the original system of three equations in a system with six ODEs:

$$2f_1 + h_1' = 0 \tag{36}$$

$$2f_2 + h_2' = 0 \tag{37}$$

$$-pf_2 + 2Ff_1 - 2Gg_1 + Hf_1' + F'h_1 - (\nu^*)'f_1' - \nu^* f_1'' = 0 \tag{38}$$

$$pf_1 + 2Ff_2 - 2Gg_2 + Hf_2' + F'h_2 - (\nu^*)'f_2' - \nu^* f_2'' = 0 \tag{39}$$

$$-pg_2 + 2Gf_1 + 2Fg_1 + Hg_1' + G'h_1 - (\nu^*)'g_1' - \nu^* g_1'' = 0 \tag{40}$$

$$pg_1 + 2Gf_2 + 2Fg_2 + Hg_2' + G'h_2 - (\nu^*)'g_2' - \nu^* g_2'' = 0. \tag{41}$$

Boundary conditions applicable to the perturbation and given by Eq. 18 are rewritten to take into account the splitting of the perturbation in real and imaginary parts requires boundary conditions applicable to the real and imaginary parts:

$$\begin{aligned} &f_1(0) = f_2(0) = h_1(0) = h_2(0) = 0 \\ &g_1(0) = 1 \\ &g_2(0) = 0 \\ &f_1(\infty) = f_2(\infty) = g_1(\infty) = g_2(\infty) = 0 \end{aligned} \tag{42}$$

Solving the equations of the unsteady problem requires the previous knowledge of the steady profiles F, G and H, namely the steady behaviour of the system.

We assume first that no viscosity gradient exists and we have $\nu^* = 1$ and $(\nu^*)' = 0$. In this situation profiles F, G and H, used to solve the unsteady equations (Eqs. 36-41) are the steady ones obtained by solving the hydrodynamic equations decoupled from the mass transfer equation (Eqs. 11-13). The resulting $\tilde{f}$, $\tilde{g}$ and $\tilde{h}$ profiles are those obtained by Tribollet & Newman [5] up to the third digit. Differences appear in the fourth digit and are probably due to different truncation errors.

Next, we address the case where a previously specified viscosity gradient exists, given by Eq. 19, and depending on the axial coordinate ξ only. As in the previous case, both the steady problem, obeying Eqs. 11-13, and unsteady one, obeying Eqs. 36-41 are solved using the hydrodynamic equations only. However, now we have $\nu(0) \neq \nu(\infty)$, so the results depend on the interfacial value of the viscosity gradient. Comparison with the results obtained for the case where the concentration and the hydrodynamic fields are coupled through the viscosity we use $\nu(0)/\nu(\infty)$ values given in Table 1. The viscosity profile given by Eq. 19 independs of the Schimidt number, so does the whole methodology adopted for this case. However, the values obtained for $\tilde{f}'(0, p)/\tilde{f}'(0, 0)$ as functions of the nondimensional modulating frequency $p = \omega/\Omega$ refer to $Sc(\infty) = 1500$, 2000 and 2200 respectively, through the values of the ratio $\nu(0)/\nu(\infty)$ given in Table 1, used in the calculations.

As the modulation frequency vanishes Eq. 6 shows that, as the modulating frequency vanishes $rf_1(\xi)$ tends to the direction of the derivative of v_r with respect to Ω and Eq. 39 shows that f_2' goes to zero. In consequence we have that $\tilde{f}_1(0, 0) = \frac{3}{2}F'(0)$. By using the value of $F'(0)$ obtained for the steady state case we find $\tilde{f}'(0, 0) = 0{,}76523565$. This value is used to evaluate the normalized amplitude of $\tilde{f}'$ in Tables 2, 4 and 6, with the viscosity profile given by Eq. 19.

Finaly, we consider the case where the steady state functions F, G and H used in the evaluation of the unsteady hydrodymamic field were obtained with the hydrodynamic and the mass transfer equations coupled through the viscosity. Now, the governing equations of the steady velocity field (Eqs. 11-13 and 24) depend on the Schmidt number. Values assigned to $Sc(\infty)$ and $\nu(0)/\nu(\infty)$ are the ones given in Table 1. Results for $\tilde{f}'(0, p)/\tilde{f}'(0, 0)$ as functions of the non dimensional modulating frequency $p = \omega/\Omega$ are shown in Tables 3, 5 and 7, for $Sc(\infty) = 1500$, 2000 and 2200, respectively. Evaluation of the normalized amplitude $\tilde{f}'$ presented in these tables assume the same value $\tilde{f}'(0, 0)$ previously used in Tables 2, 4 and 6, namely, 0,76523565.

By using the results obtained with constant viscosity (same results obtained by Tribollet & Newman [5]) and data from Tables 4 and 5 we present graphically the values of the hydrodynamic transfer function *versus* nondimensional frequency p in Figure 1 for cases with constant viscosity, variable viscosity but concentration and hydrodynamic fields uncoupled and coupled fields. Results associated to Tables 2 and 3, as well as those associated to Tables 6 and 7 are similar to those presented in Figure 1 and not showed graphically.

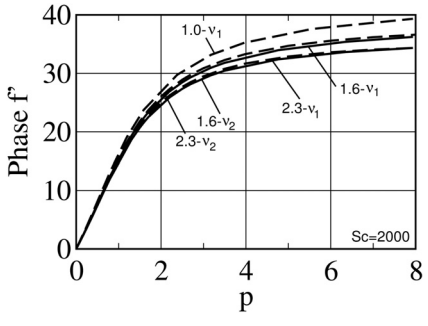

Figure 1 – $\tilde{f}'(0, p)/\tilde{f}'(0, 0)$ for $Sc = 2000$, and $\nu(0)/\nu(\infty) = 1$, 1.6 and 2.3 with concentration and hydrodynamic fields uncoupled (ν_1) and with coupled fields (ν_2), and $\nu(0)/\nu(\infty) = 1.6$ and 2.3.

Figure 1 shows that, independently of the existence or not of a viscosity gradient and of the existence or not of coupling between concentration an the hydrodynamic fields, the phase tends to a limit value of 45°. However, when a viscosity gradient exits, the phase limit value is attained at nondimensional frequency value p higher than in cases of constant viscosity. And the results show that the phase delay increases as the viscosity gradient increases, both for the uncoupled and coupled cases. Comparison between coupled and uncoupled cases for same $\nu(0)/\nu(\infty)$ ratio shows larger values phase for the coupled up to a contain limit value of p and approximately the same phase values for both the uncoupled and coupled cases beyond that threshold value of p.

Figure 2 presents the results for the hydrodynamic transfer function obtained with coupled concentration and hydrodynamic fields, $\nu(0)/\nu(\infty) = 2.5$ and three Schmidt number values.

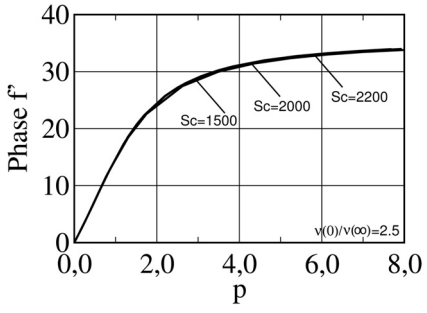

Figure 2 – $\tilde{f}'(0, p)/\tilde{f}'(0, 0)$ for $\nu(0)/\nu(\infty) = 2.5$, and $Sc = 1500, 2000$ and 2200 with coupled concentration and hydrodynamic fields.

As shown in Figure 2, an increase in the Schmidt number for prescribed p results in higher values of the phase. The results for $\nu(0)/\nu(\infty) = 1.8$ are similar and not presented graphically here. We remind that the Schmidt number affects the results obtained in the uncoupled case only when the ratio $\nu(0)/\nu(\infty)$ changes, since the viscosity profile given by Eq. 19 is independent of Sc. We addressed this case for purposes of comparison with the results obtained with the concentration an hydrodynamic fields coupled.

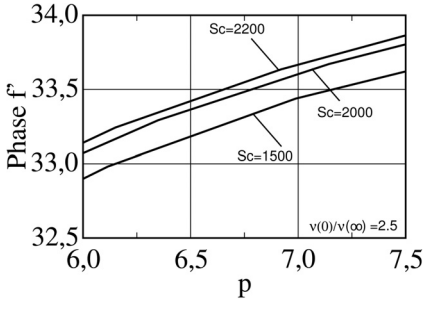

Figure 3 – Curves of the Figure 2 only for the region of high values of p.

In both cases considered, namely by increasing either the ratio $\nu(0)/\nu(\infty)$ at constant Schmidt number, or the Schmidt number at constant values of $\nu(0)/\nu(\infty)$, an increase in the electrolyte viscosity close to the RDE occurs. In this sense, we can consider an increase in the perturbation frequency as equivalent to placing a perturbation source closer to the RDE surface. A viscosity increase leads thus to an equivalent result to the one obtained by imposing a higher perturbation frequency to the angular velocity of the RDE. Inconsequence, a prescribed phase delay of the system response is attained at frequencies that decrease with the system viscosity.

Table 2 – $\tilde{f}'(0,\, p)/\tilde{f}'(0,0)$ in polar coordinates *vs.* the dimensionless frequency, $p\, Sc^{1/3}$, for $Sc = 1500$ and viscosity profile given by Eq. 19.

	$\nu(0)/\nu(\infty) = 1.8$		$\nu(0)/\nu(\infty) = 2.5$	
$p\, Sc^{1/3}$	$\mathrm{A}(p,0)/\mathrm{A}(0,0)$	$\theta(^\circ)$	$\mathrm{A}(p,0)/\mathrm{A}(0,0)$	$\theta(^\circ)$
0	1.000000	0.0000000	1.000000	0.0000000
1	0.946568	15.489414	0.947228	14.997014
2	0.804020	25.707100	0.807421	24.778825
3	0.690411	30.428458	0.696314	29.188066
4	0.611836	32.783329	0.619617	31.311666
5	0.555477	34.112250	0.564680	32.459186
6	0.512982	34.939189	0.523297	33.137469
7	0.479582	35.492284	0.490793	33.564869
8	0.452466	35.882727	0.464417	33.846586
10	0.410703	36.388426	0.423814	34.171395
20	0.305300	37.228397	0.321381	34.468995
40	0.228370	37.649495	0.246444	34.429723
60	0.193106	37.962198	0.211869	34.549563
80	0.171498	38.289904	0.190515	34.790205
100	0.156390	38.630073	0.175461	35.096970

Table 3 – $\tilde{f}'(0,\, p)/\tilde{f}'(0,0)$ in polar coordinates *vs.* the dimensionless frequency, $p\, Sc^{1/3}$, for $Sc = 1500$ and viscosity profile given by Eq. 27.

	$\nu(0)/\nu(\infty) = 1.8$		$\nu(0)/\nu(\infty) = 2.5$	
$p\, Sc^{1/3}$	$\mathrm{A}(p,0)/\mathrm{A}(0,0)$	$\theta(^\circ)$	$\mathrm{A}(p,0)/\mathrm{A}(0,0)$	$\theta(^\circ)$
0	1.000000	0.000000	1.000000	0.000000
1	0.947738	15.149616	0.948610	14.653529
2	0.808337	25.141212	0.812343	24.227568
3	0.697036	29.780154	0.703763	28.590333
4	0.619888	32.126939	0.628580	30.747393
5	0.564415	33.485750	0.574546	31.967209
6	0.522474	34.363442	0.533694	32.737847
7	0.489417	34.979386	0.501487	33.268291
8	0.462500	35.439862	0.475250	33.658648
10	0.420864	36.096492	0.434630	34.206791
20	0.314189	37.686691	0.330103	35.538455
40	0.233678	39.206731	0.250192	36.938783
60	0.195607	40.192083	0.211782	37.921856
80	0.171921	40.928981	0.187583	38.683701
100	0.155263	41.511128	0.170394	39.296979

Table 4 – $\tilde{f}'(0, p)/\tilde{f}'(0, 0)$ in polar coordinates *vs.* the dimensionless frequency, $p\,Sc^{1/3}$, for $Sc = 2000$ and viscosity profile given by Eq. 19.

	$\nu(0)/\nu(\infty) = 1.6$		$\nu(0)/\nu(\infty) = 2.3$	
$p\,Sc^{1/3}$	$A(p, 0)/A(0, 0)$	$\theta(^\circ)$	$A(p, 0)/A(0, 0)$	$\theta(^\circ)$
0	1.000000	0.0000000	1.000000	0.0000000
1	0.946337	15.663770	0.947058	15.122822
2	0.802827	26.036009	0.806546	25.015876
3	0.688345	30.868398	0.694795	29.504592
4	0.609118	33.305872	0.617613	31.686922
5	0.552268	34.699814	0.562308	32.880401
6	0.509391	35.580187	0.520636	33.596275
7	0.475684	36.178564	0.487899	34.055411
8	0.448316	36.608239	0.461330	34.364550
10	0.406160	37.179316	0.420423	34.734921
20	0.299778	38.215452	0.317204	35.168983
40	0.222240	38.800269	0.241721	35.246523
60	0.186803	39.177567	0.206943	35.416843
80	0.165160	39.530819	0.185502	35.681706
100	0.150078	39.877073	0.170416	35.999275

Table 5 – $\tilde{f}'(0, p)/\tilde{f}'(0, 0)$ in polar coordinates *vs.* the dimensionless frequency, $p\,Sc^{1/3}$, for $Sc = 2000$ and viscosity profile given by Eq. 27.

	$\nu(0)/\nu(\infty) = 1.6$		$\nu(0)/\nu(\infty) = 2.3$	
$p\,Sc^{1/3}$	$A(p, 0)/A(0, 0)$	$\theta(^\circ)$	$A(p, 0)/A(0, 0)$	$\theta(^\circ)$
0	1.000000	0.000000	1.000000	0.000000
1	0.947167	15.408136	0.948111	14.854365
2	0.805933	25.604425	0.810321	24.581515
3	0.693147	30.364827	0.700530	29.028340
4	0.614986	32.785404	0.624538	31.231319
5	0.558813	34.191358	0.569954	32.476500
6	0.516372	35.100124	0.528717	33.260568
7	0.482947	35.736757	0.496233	33.797037
8	0.455754	36.210843	0.469795	34.188584
10	0.413747	36.880985	0.428917	34.730321
20	0.306644	38.438428	0.324218	35.979022
40	0.226693	39.833036	0.244967	37.233659
60	0.189278	40.730160	0.207192	38.134868
80	0.166134	41.412244	0.183482	38.854073
100	0.149912	41.961363	0.166668	39.447073

Table 6 – $\tilde{f}'(0,\, p)/\tilde{f}'(0,0)$ in polar coordinates *vs.* the dimensionless frequency, $p\, Sc^{1/3}$, for $Sc = 2200$ and viscosity profile given by Eq. 19.

	$\nu(0)/\nu(\infty) = 1.2$		$\nu(0)/\nu(\infty) = 1.7$	
$p\, Sc^{1/3}$	$\mathrm{A}(p,0)/\mathrm{A}(0,0)$	$\theta(^\circ)$	$\mathrm{A}(p,0)/\mathrm{A}(0,0)$	$\theta(^\circ)$
0	1.000000	0.0000000	1.000000	0.0000000
1	0.945784	16.083688	0.946455	15.574181
2	0.799969	26.828231	0.803439	25.866999
3	0.683408	31.928437	0.689406	30.642316
4	0.602637	34.565610	0.610512	33.037314
5	0.544631	36.117066	0.553914	34.397808
6	0.500860	37.127087	0.511232	35.250685
7	0.466439	37.835455	0.477683	35.825758
8	0.438486	38.360502	0.450443	36.235236
10	0.395428	39.090626	0.408488	36.772656
20	0.286853	40.603270	0.302604	37.707811
40	0.208072	41.578855	0.225372	38.208549
60	0.172370	42.101800	0.190019	38.552934
80	0.150759	42.504763	0.168390	38.893422
100	0.135830	42.853913	0.153292	39.236914

Table 7 – $\tilde{f}'(0,\, p)/\tilde{f}'(0,0)$ in polar coordinates *vs.* the dimensionless frequency, $p\, Sc^{1/3}$, for $Sc = 2200$ and viscosity profile given by Eq. 27.

	$\nu(0)/\nu(\infty) = 1.2$		$\nu(0)/\nu(\infty) = 1.7$	
$p\, Sc^{1/3}$	$\mathrm{A}(p,0)/\mathrm{A}(0,0)$	$\theta(^\circ)$	$\mathrm{A}(p,0)/\mathrm{A}(0,0)$	$\theta(^\circ)$
0	1.000000	0.000000	1.000000	0.000000
1	0.946172	15.954692	0.947275	15.326193
2	0.801438	26.606846	0.806497	25.449726
3	0.685692	31.664249	0.694129	30.157869
4	0.605438	34.285503	0.616283	32.539679
5	0.547765	35.835522	0.560349	33.915244
6	0.504212	36.852559	0.518096	34.799159
7	0.469935	37.573209	0.484821	35.414846
8	0.442076	38.113966	0.457753	35.870895
10	0.399108	38.881622	0.415941	36.511275
20	0.290275	40.610166	0.309323	37.983384
40	0.210477	41.941669	0.229643	39.318757
60	0.173932	42.699381	0.192264	40.203122
80	0.151681	43.252755	0.169084	40.888458
100	0.136268	43.695573	0.152798	41.447074

4 CONCLUSIONS

The following conclusion can be taken from the results above presented:

1. The existence of a viscosity gradient in the neighborhood of the RDE affects the hydrodynamic transfer function and changes increase with the increase of the perturbation frequency imposed to the angular velocity of the electrode.

2. The coupling between the concentration and the hydrodynamic fields introduces a dependency of the transfer function on the Schmidt number.

3. Higher viscosity gradients lower the phase angle delay of the transfer function for a given perturbation frequency p and a Schmidt number, in comparison with systems with constant viscosity.

4. Higher Schmidt number increase the phase angle delay of the transfer function for a given perturbation frequency p and a viscosity gradient, in comparison with systems with constant viscosity.

REFERENCES

[1] LEVICH VG. 1962. Physicochemical Hydrodynamics, Prentice Hall, Englewood Cliffs, NJ.

[2] RIDDIFORD AC. 1966. Advanced Electrochemistry and Electrochemical Engineering, Vol. 4, P. Delahay and C.W. Tobias, Editors, p. 47, Interscience, New York.

[3] ARVIA AJ & MARCHIANO SL. 1971. Modern Aspects of Electrochemistry, Vol. 6, J.O'M. Bockris and B.E. Conway, Editors, p. 159, Plenum Press, New York.

[4] NEWMAN J. 1973. Electrochemical Systems, Prentice Hall, Inc., Englewoods Cliffs, NJ.

[5] TRIBOLLET B & NEWMAN J. 1983. J. Electrochem. Soc., 130: 2016.

[6] NEWMAN J. 1968. Ind. Eng. Chem., 7: 514.

[7] BARCIA OE, MATTOS OR & TRIBOLLET B. 1992. J. Electrochem. Soc., 139: 446.

[8] BECK TR. 1982. J. Electrochem. Soc., 129: 2412.

[9] PODESTA JJ, PIATTI RCV & ARVIA AJ. 1979. J. Electrochem. Soc., 126: 1363.

[10] JENKIN HDB & MARCUS Y. 1995. Chem. Rev. (Washington, D.C.), 95: 2695.

[11] ESTEVES MJC, CARDOSO MJEM & BARCIA OE. 2002. Ind. Eng. Chem. Res., 41: 5109.

[12] CALABRESE BARTON S & WEST AC. 2001. J. Electrochem. Soc., 148: A381.

[13] BARCIA OE, MANGIAVACCHI N, MATTOS OR, PONTES J & TRIBOLLET B. 2008. J. Electrochem. Soc., 155: D424.

[14] PONTES J, MANGIAVACCHI N, BARCIA OE, MATTOS OR & TRIBOLLET B. 2007. Phys. Fluids, 19: 114109.

[15] VON KÁRMÁN T. 1921. Z. Angew. Math. Mech., 1: 233.

[16] ORAZEM ME & TRIBOLLET B. 2008. In: Electrochemical Impedance Spectroscopy, John Wiley & Sons, New Jersey.

[17] FERREIRA JRRM, BARCIA OE, MATTOS OR & TRIBOLLET B. 1994. Electrochim. Acta, 39: 933.

[18] GERALDO AB, BARCIA OE, MATTOS OR, HUET F & TRIBOLLET B. 1998. Electrochim. Acta, 44: 455.

[19] ABRAMOWITZ M & STEGUN IA (Eds.). 1972. Handbook of Mathematical Functions with Formulas, Graphs, and Mathematical Tables. New York: Dover.

[20] ORAZEM ME & TRIBOLLET B. 2008. Electrochemical Impedance Spectroscopy, Volume 48 de The ECS Series of Texts and Monographs. Editora Wiley.